Research Article

Magnet-targeted delivery of bone marrow-derived mesenchymal stem cells improves therapeutic efficacy following hypoxic-ischemic brain injury

https://doi.org/10.4103/1673-5374.310942

Date of submission: July 13, 2020

Date of decision: September 28, 2020

Date of acceptance: January 28, 2021

Date of web publication: March 25, 2021

Chuang Sun[1, #], Ao-Dan Zhang[1, #], Hong-Hai Chen[1], Jie Bian[1, *], Zheng-Juan Liu[2, *]

Graphical Abstract *Superparamagnetic iron oxide nanoparticles and poly-L-lysine (SPIO-PLL)-labeled bone marrow-derived stem cells (BMSCs) therapy repairs the damage induced by hypoxic-ischemic brain damage (HIBD) in rats*

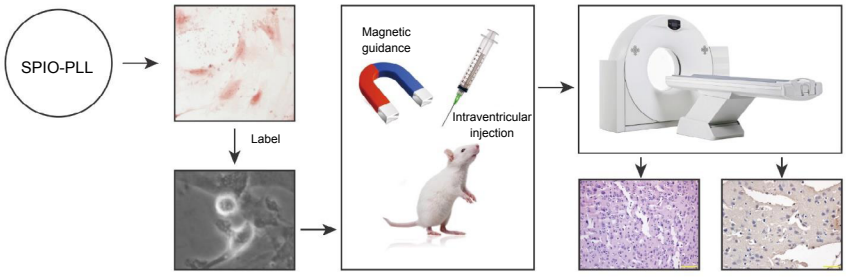

Abstract

Stem cell transplantation may represent a feasible therapeutic option for the recovery of neurological function in children with hypoxic-ischemic brain injury; however, the therapeutic efficacy of bone marrow-derived mesenchymal stem cells largely depends on the number of cells that are successfully transferred to the target. Magnet-targeted drug delivery systems can use a specific magnetic field to attract the drug to the target site, increasing the drug concentration. In this study, we found that the double-labeling using superparamagnetic iron oxide nanoparticle and poly-L-lysine (SPIO-PLL) of bone marrow-derived mesenchymal stem cells had no effect on cell survival but decreased cell proliferation 48 hours after labeling. Rat models of hypoxic-ischemic brain injury were established by ligating the left common carotid artery. One day after modeling, intraventricular and caudal vein injections of 1×10^5 SPIO-PLL-labeled bone marrow-derived mesenchymal stem cells were performed. Twenty-four hours after the intraventricular injection, magnets were fixed to the left side of the rats' heads for 2 hours. Intravoxel incoherent motion magnetic resonance imaging revealed that the perfusion fraction and the diffusion coefficient of rat brain tissue were significantly increased in rats treated with SPIO-PLL-labeled cells through intraventricular injection combined with magnetic guidance, compared with those treated with SPIO-PLL-labeled cells through intraventricular or tail vein injections without magnetic guidance. Hematoxylin-eosin and terminal deoxynucleotidyl transferase dUTP nick-end labeling (TUNEL) staining revealed that in rats treated with SPIO-PLL-labeled cells through intraventricular injection under magnetic guidance, cerebral edema was alleviated, and apoptosis was decreased. These findings suggest that targeted magnetic guidance can be used to improve the therapeutic efficacy of bone marrow-derived mesenchymal stem cell transplantation for hypoxic-ischemic brain injury. This study was approved by the Animal Care and Use Committee of The Second Hospital of Dalian Medical University, China (approval No. 2016-060) on March 2, 2016.

Key Words: bone marrow-derived mesenchymal stem cells; cell apoptosis; diffusion coefficient; cell labeling; intraventricular injection; intravoxel incoherent motion; magnetic guidance; perfusion fraction; superparamagnetic nanoparticles

Chinese Library Classification No. R454; R742; Q482.54

Introduction

Hypoxic-ischemic brain damage (HIBD) is a common cause of neonatal ischemic brain damage and a major cause of severe neurological disorders in children (Walton et al., 1999; Jiang et al., 2020). Each year, four million infants among 130 million newborns worldwide suffer from HIBD, which is associated with one million deaths due to brain injury (Liu et al., 2016). Furthermore, an additional one million patients suffer serious long-term sequelae, including neurodevelopmental disorders (Yıldız et al., 2017). At present, no specific treatment has been developed for HIBD.

Previous studies have demonstrated that neural stem cells exist in some areas of the brain, and brain injury caused by hypoxia can stimulate neural stem cell proliferation and differentiation to restore some neural functions (Murnane et al., 1994; Evangelou et al., 2000; Lin and Chen, 2020). However, the number of neural stem cells is very limited, and endogenous neural stem cells have a very limited capability to alleviate neurological impairments in HIBD. In the fields of tissue engineering and cell- and gene-based therapies, bone

[1]Department of Radiology, The Second Hospital of Dalian Medical University, Dalian, Liaoning Province, China; [2]Department of Pediatrics, The Second Hospital of Dalian Medical University, Dalian, Liaoning Province, China

***Correspondence to:** Jie Bian, PhD, Curl1@163.com; Zheng-Juan Liu, PhD, Liuzj625@163.com.

https://orcid.org/0000-0002-9104-3588 (Jie Bian)

#Both authors contributed equally to this work.

How to cite this article: *Sun C, Zhang AD, Chen HH, Bian J, Liu ZJ (2021) Magnet-targeted delivery of bone marrow-derived mesenchymal stem cells improves therapeutic efficacy following hypoxic-ischemic brain injury. Neural Regen Res 16(11):2324-2329.*

marrow-derived mesenchymal stem cells (BMSCs) are the most widely used cell type explored as a potential therapeutic tool (Lee et al., 2006; Phillips et al., 2013).

The damaged integrity of the blood-brain barrier during brain injury provides a structural pathway through which BMSCs can enter the central nervous system by leveraging the function of the circulatory or brain ventricular systems. The therapeutic effects of BMSCs largely depend on the number of BMSCs that are effectively translocated to the target site. BMSC transplantation has been shown to promote the functional recovery of ischemic tissues and improve the learning and memory abilities in HIBD patients (Krampera et al., 2006). However, tracing BMSCs and monitoring their movement and location is currently very difficult to perform. Magnetically targeted drug delivery is a new drug delivery technique that has increased in popularity in recent years and primarily consists of magnetic particles, drugs, and drug carriers. In a magnetically targeted drug delivery system, drugs that exhibit a response to a specific magnetic field can be magnetically maneuvered to the target site, increasing the concentration of the drugs at the target location and reducing toxicity and side effects due to reduced off-target effects (Lidsky et al., 2012).

At present, the most widely used magnetic particles are superparamagnetic iron oxide (SPIO) particles, which are characterized by a small diameter (10–20 nm), a large specific surface area, high permeability, and magnetic induction intensity. SPIO particles exist in the form of a single domain structure, featuring superparamagnetism, low toxicity, and high biocompatibility (Sala et al., 2010). Recent studies have focused on the magnetic targeting of drug delivery to improve the efficacy of chemotherapy drugs in cancer treatments, and several studies have confirmed the efficiency of this approach (Lidsky et al., 2012). SPIO is a magnetic resonance imaging (MRI) contrast agent and, more specifically, SPIO coated with carboxydextran or dextran are particularly popular and have been approved by the U. S. Food and Drug Administration for clinical use (Lee et al., 2006). The SPIO labeling of specific cells can be used to assess molecule distribution, migration, and trafficking from the blood to the target site in the brain.

Intravoxel incoherent motion (IVIM) is a diffusion-weighted MRI sequence that uses multi-b-value diffusion-weighted imaging with bi-exponential curve fitting. IVIM was first described by Le Bihan in the 1980s and is used to estimate the changes in the perfusion parameters of a hypoxic-ischemic brain state with high sensitivity (Le Bihan et al., 1988). Using this technique, we can quantitatively analyze two types of water molecule movement, including diffusion and microcirculation perfusion. In recent years, the *in vivo* IVIM technique has been applied for various clinical assessments, especially in studies focusing on molecular movements in the brain (Fung et al., 2011; Federau et al., 2014).

In this study, we designed a new type of SPIO-labeled BMSC and used a magnetically targeted drug delivery approach to monitor the distribution and migration of BMSCs and evaluated the therapeutic effects when these cells were administered to a rat model of HIBD.

Materials and Methods

Isolation, culture, and identification of BMSCs

This study was approved by the Institutional Animal Care and Use Committee of The Second Hospital of Dalian Medical University, China (No. 2016-060) on March 2, 2016. Specific-pathogen-free Sprague-Dawley rats, 6–8 weeks old, were used for BMSC isolation. Eighty newborn, male, Sprague-Dawley rats, 7 days old, were used for the animal experiments. All rats were provided by the Animal Experimental Center of Dalian Medical University (license No. SCXK (Liao) 2018-0003).

Adult rats were anesthetized by intraperitoneal injection of 3% pentobarbital (West Chemical, Linyi, China) at 30 mg/kg. Under sterile conditions, the femur and tibia were separated. After the muscle, tendon, and connective tissues were removed, the bone marrow cavity was exposed and rinsed three times with low-glucose Dulbecco's modified Eagle medium to harvest the BMSC cell suspensions. Cells were filtered through a 200 mesh cell filter and centrifuged at 1000 r/min for 5 minutes and resuspended in Dulbecco's modified Eagle medium supplemented with 20% fetal bovine serum and cultured at 37°C in a 5% CO_2 incubator. The culture medium was replaced after 24 hours to remove cell debris and non-adherent cells. The culture medium was subsequently replaced every 2 to 3 days. When cells reached approximately 80% confluence, BMSCs were passaged with 0.25% trypsin to dissociate adherent cells (Westerweel and Verhaar, 2008).

Flow cytometry was used to detect the expression of CD29, CD90, CD45, and CD11b on the cell surface to identify BMSCs (Miao et al., 2006), using the following reagents: fluorescein isothiocyanate-IgG (1:100), phycoerythrin (PE)-IgG (1:100), PE-CD29 monoclonal antibody (1:100), PE-CD11b monoclonal antibody (1:40), PE-Cy5-CD44 monoclonal antibody (1:20), and anti-mouse fluorescein isothiocyanate stem cell antigen-1 (1:20). After incubation at 37°C for 20 minutes, 1 mL 0.9% normal saline was added, and the cells were resuspended and subjected to flow cytometry analysis (BD Biosciences, San Jose, CA, USA).

HIBD rat model

Newborn rats were divided into five groups (n = 16): the sham group (Sham), the HIBD group, HIBD rats treated with SPIO-PLL-labeled BMSCs by intraventricular injection (SPIO-PLL ic.), HIBD rats treated with SPIO-PLL-labeled BMSCs by intraventricular injection under magnetic guidance (SPIO-PLL ic. + MG), and HIBD rats treated with SPIO-PLL-labeled BMSCs by tail vein injection (SPIO-PLL tv.). The rats were housed at a controlled temperature of 22–25°C under a 12-hour light-dark cycle. The HIBD model was induced as previously described (Yager, 2004). Briefly, the newborn rats were anesthetized with 2% sevoflurane (Hengrui Pharmaceutical, Shanghai, China) at a rate of 300 mL/min, which was maintained during the operation. The left common carotid artery was exposed, carefully separated, and closed with a double line ligation. After the operation, the rats recovered for 30 minutes in an oxygen-deficient, heated box, and maintained at 37°C for 2 hours. The concentration of oxygen was controlled at 8% (7–9%) and monitored using an oxygen monitor throughout the entire process. The humidity was 70 ± 5%. In the sham group, the left common carotid artery was separated but not ligated, and the wound was subsequently sutured without anoxia treatment.

BMSC labeling with SPIO poly-L-lysine

SPIO and PLL (Sofe Biomedicine, Shanghai, China) were added to Dulbecco's modified Eagle medium at final concentrations of 50 μg/mL SPIO and 1.5 μg/mL PLL. After shaking for 60 minutes at room temperature, a mixture of SPIO-PLL was obtained for use in further experiments. The SPIO-PLL mixture was diluted with an equal volume of medium to obtain final concentrations of 25 μg/mL SPIO and 0.75 μg/mL PLL. Cells were maintained at 37°C and incubated with SPIO-PLL mixture at 5% CO_2 for 24 hours. BMSCs labeled with SPIO-PLL were fixed in 4% paraformaldehyde solution for 15 minutes, followed by the addition of Perls staining solution (Solarbio Life Sciences, Beijing, China) and incubation in a 37°C incubator for 30 minutes. The SPIO-PLL labeling efficiency of BMSCs was observed under a microscope. The cell suspension was mixed with 0.4% trypan blue solution (Shanghai Westang Bio-Tech Co., Shanghai, China) at a rate of 9:1. Within 3 minutes,

dead cells were stained a clear blue, and live cells remained clear and colorless under microscopic examination. The cell proliferation rate was examined (Zuo et al., 2019) using 3-(4,5-dimethylthiazol-2-yl)-2,5-diphenyltetrazolium bromide (MTT, Sigma, Santa Clara, CA, USA) before and after SPIO-PLL labeling to determine whether SPIO-PLL labeling affected cell proliferation. BMSCs were incubated with MTT reagent (0.5 mg/mL, final concentration) for 4 hours at 37°C and 5% CO_2. The optical density at 570 nm was observed using an inverted phase-contrast microscope (Mike Audi, Xiamen, China).

Intraventricular and caudal vein injections of SPIO-labeled BMSCs

One day after establishing the HIBD rat model, intracranial injections were performed, guided by a stereotaxic brain atlas (Zuo et al., 2019). Rats were anesthetized and fixed in a stereotaxic instrument. The injection site was determined according to a brain stereotaxic atlas (relatively to the anterior fontanelle, anteroposterior [AP] = –0.9 mm, dorsoventral [DV] = –3.5 mm, mediolateral [ML] = –1.5 mm). The skull was broken with a bone drill, the dura mater was punctured with a syringe needle, and 5 μL of the cell suspension (containing approximately 1×10^5 cells) was injected with a micro-syringe (RWD Life Science, Shenzhen, China) at a speed of 1 μL/min. After injection, the needle was left in place for 5 minutes and then removed. The injection site was sealed with bone wax, and the wounds were sutured. At 24 hours after intraventricular injections, an iron boron magnet with a magnetic field intensity of 3900 gauss was fixed to the extracranial site of the HIBD rat model using tape. Magnets were affixed for 2 hours in the magnetic guidance group, without anesthetization.

For the caudal vein injection of SPIO-PLL-labeled BMSCs, the tail vein was sterilized and subsequently injected with 5 μL of cell suspension (containing approximately 1×10^5 cells) using a microsyringe. Indwelling needles were inserted into the tail veins on both sides of the tail to inject the cell suspension, which was followed by 1 mL normal saline for wash out.

***In vivo* tracing of BMSCs after injection**

After BMSC transplantation, the rats were examined via MRI (Siemens Verio 3.0T MRI system, Erlangen, Bavaria Land, Germany) at 1-, 2-, 3- and 4-week post-transplantation. The scanning sequence included T1-weight images (T1WI), T2-weighted images (T2WI), T2-fluid-attenuated inversion recovery (FLAIR), and multiple B-value diffusion-weighted imaging (Wang et al., 2011). After the original IVIM image was transformed with the ImageJ software (National Institutes of Health, Bethesda, MD, USA), the brain region of interest was identified in the T1WI and applied to all other image types. Information from each region of interest was manually plotted and measured; each region of interest was measured three times using four individual elements. The animals were re-examined one week later, and the average values of the repeated measurements were evaluated using the F value (perfusion fraction) and D value (pure diffusion coefficient). The D value represents the diffusion movement of pure water (slow diffusion movement), which excludes the influence of microcirculation perfusion associated with the capillary network on diffusion in the tissue structure. More restricted diffusion of water molecules corresponded with a lower D value (Federau et al., 2014).

Pathological observations

After MRI, the rats were anesthetized with pentobarbital at 30 mg/kg, perfused with saline, and fixed with 4% paraformaldehyde. The brains were harvested and the tissue was dehydrated with alcohol and embedded in xylene and paraffin wax, before being cut into sections of 5 μm thickness. After being dehydrated with alcohol, the sections were stained with hematoxylin (Solarbio Life Sciences) and differentiated in 1% hydrochloric acid alcohol (Sinopharm, Beijing, China). Distilled water was used for anti-blue staining. The sections were stained with eosin (Sinopharm) and then dehydrated with alcohol. The sections were permeated with xylene (Sinopharm) and sealed with gum. The slides were observed under a microscope (Olympus, Tokyo, Japan).

To perform the 3,3′-diaminobenzidine staining, sections were permeated with 0.1% Triton X-100 (0.1% sodium citrate, Beyotime, Shanghai, China), and 3% H_2O_2 (Sinopharm) was used for penetration. The terminal deoxynucleotidyl transferase dUTP nick-end labeling (TUNEL) reaction solution (Wanleibio, Shenyang, Liaoning Province, China) was used for enzyme labeling. 3,3′-Diaminobenzidine substrate (Solarbio Life Sciences) was used for color development. To perform hematoxylin staining (Solarbio Life Sciences), 1% hydrochloric acid ethanol was used for anti-blue staining. Neutral balsam was added to seal the sections. Staining was observed under a microscope (Olympus) (Walton et al., 1999). Pathological images were observed and captured with an Olympus IX51 microscope.

Statistical analysis

SPSS 21.0 software (IBM SPSS, Inc., Chicago, IL, USA) was used to perform statistical analyses of the experimental data. All data are expressed as the mean ± standard deviation (SD). Student's *t*-test was used to determine the significance of differences between two groups. One-way analysis of variance with Dunnett's *post hoc* test was used to analyze differences in the IVIM analyses. $P < 0.05$ was considered significant.

Results

Effects of SPIO-PLL labeling on the survival and proliferation of BMSCs

After isolation, BMSCs were labeled with SPIO-PLL (**Figure 1A**). The BMSCs were CD29 [integrin family antigen marker VLAβ (Shen et al., 1991)] and CD90 [cell adhesion molecule immunoglobulin Thy-1 (Leyton et al., 2019)] positive and CD45 [Pan leukocyte marker antigen (Hendrickx and Bossuyt, 2001)] and CD11b [myeloid lymphocyte surface antigen Mac1 (Diamond and Springer, 1993)] negative (**Figure 1B**). These results showed that the isolated cells were derived from bone marrow-derived mesenchymal components.

After SPIO-PLL labeling, BMSCs were further identified by Prussian blue staining (**Figure 2A**). The cell survival rate of BMSCs after SPIO-PLL labeling did not differ significantly before and after SPIO-PLL labeling (83% *vs*. 93%, $P = 0.06$). As shown in **Figure 2B** and **C**, the MTT results indicated no significant difference in cell proliferation 24 hours post-SPIO-PLL labeling ($P = 0.58$); however, at 48 hours after labeling, the cell proliferation rate of SPIO-PLL-labeled cells decreased significantly ($P < 0.01$), indicating that SPIO-PLL labeling had an inhibitory effect on cell proliferation.

Migration effects of SPIO-PLL-labeled BMSCs in HIBD rats

The HIBD group showed the most significant diffusion limitation effects on water molecules over time (data not shown). The D values of SPIO-PLL-labeled BMSCs administered by both intraventricular and tail vein injections decreased over time, and the reduction observed for the tail vein injection group was more significant than that observed for the intraventricular injection group. In the magnetic guidance group, the D value gradually increased, although the effect was not significant. Compared with those in the HIBD group, the D and F values for the tail vein injection, intraventricular injection, and magnetic guidance groups were significantly higher ($P < 0.05$). The D values in the intraventricular injection

and magnetic guidance groups were significantly higher than that in the tail vein injection group ($P < 0.05$), and F values in the intraventricular injection and magnetic guidance groups were significantly lower than that in the tail vein injection group ($P < 0.05$). The D and F values in the magnetic guidance group were significantly higher than those in the intraventricular injection group ($P < 0.05$; **Figure 3**). These results suggest that the intraventricular injection of SPIO-PLL-labeled BMSCs under magnetic guidance conditions achieved the best therapeutic effect.

Effects of BMSC treatment on pathological changes in the HIBD rat brain

To confirm the establishment of the HIBD model, we examined the morphological changes and the rate of apoptosis in the brains of HIBD rats. Overall, we observed more extensive cerebral edema, increased inflammatory responses, and a large degree of cell death in the brains of HIBD rats relative to the sham group (**Figures 4** and **5**). SPIO-PLL-labeled BMSCs injected intraventricularly or through the tail vein promoted the recovery of neural functions and decreased the rate of cell death in all three groups (**Figures 4** and **5**). To examine differences associated with the various SPIO-PLL-labeled BMSC delivery routes, we observed that the intraventricular injection of SPIO-PLL-labeled BMSCs significantly decreased the rate of cell apoptosis compared with the tail veil injection of SPIO-PLL-labeled BMSCs. The degree of edema in the pathological tissue was reduced during the early stages of treatment, and the apoptosis rate was slightly reduced in the group that received SPIO-PLL-labeled BMSCs by intraventricular injection under magnetic guidance. During the later stages of treatment, the degree of cerebral edema in the pathological tissue was significantly reduced, and cell apoptosis was hardly observed in the magnetic guidance group (**Figures 4** and **5**).

Discussion

Cerebral edema is one of the most prominent changes that occur in HIBD. The occurrence, development, and severity of brain injury are closely related to the prognosis of the disease (Yıldız et al., 2017). The results of the current study demonstrated that the proposed method for the transplantation of SPIO-PLL-labeled BMSCs was suitable for the treatment of HIBD. This new method for the magnetic targeting of BMSCs showed more effectiveness and was advantageous for the treatment of HIBD compared with BSMCs injected by lateral ventricle injection or caudal vein injection. Overall, we show that IVIM MRI technology can be used to evaluate the therapeutic effects of SPIO-PLL-labeled BMSCs in HIBD model rats.

The treatment of brain injury using BMSCs has aroused extensive attention. Traditional BMSC delivery methods typically involve the injection of cells through the lateral ventricle, the tail vein, and the peritoneum (van Velthoven et al., 2010). In contrast to intracerebroventricular injection, several disadvantages are associated with peripheral BMSC administration (e.g., caudal vein injection), including the necessity of cells injected peripherally crossing the blood–brain barrier from the circulatory system to reach the target implantation site (van Velthoven et al., 2013). In the present study, we found that the intracerebroventricular injection method was the most effective method for the treatment of HIBD, including the successful delivery of SPIO-PLL-labeled cells to the target site and the alleviation of pathological changes.

IVIM technology was used to quantitatively analyze two separate components: the diffusion and perfusion of water molecules (Pang et al., 2013). IVIM not only provided quantitative parameters for the movement of water molecules in the brain but also reflected brain tissue perfusion conditions (Giannarini et al., 2012). When signals from extravascular water are suppressed, IVIM becomes very sensitive to changes in the blood flow and has the potential to detect changes to the blood flow rate, which is associated with neuronal activation and can also be used for the pathological assessment of stroke. A study was performed using IVIM imaging to examine 17 patients with acute stroke, which found that the F value of the perfusion fraction was significantly reduced after stroke (Federau et al., 2014; Sun et al., 2014). IVIM imaging can also evaluate the hemodynamic conditions of the microvasculature and reflect ischemia and hypoxia in tissues. Compared with traditional diffusion-weighted imaging technology, IVIM can more accurately reflect the diffusion movement of molecules in the brain. IVIM perfusion parameters can reflect vasoconstriction in hyperoxia and vasodilation in hypercapnia (Shinmoto et al., 2012). Accordingly, IVIM can be an effective and promising imaging technique for the quantitative analysis of cerebral perfusion when investigating neurological diseases (Luciani et al., 2008).

To explore the effects of SPIO-PLL-labeled BMSCs, a pathological analysis was performed. The death of neurons in HIBD is typically caused by necrosis and apoptosis, and these two pathways are characterized by significant differences in morphological and biochemical changes and are regulated by different pathways (van Velthoven et al., 2010; Xue et al., 2020). The neuronal necrosis is typically observed at the center of ischemic areas, whereas apoptosis is usually observed in the marginal areas of the affected region in the HIBD brain. Therefore, necrotic neurons are not easily saved, but apoptotic cells can be rescued via modifications of the upstream signaling pathways. In this study, the results of hematoxylin/eosin and TUNEL staining in HIBD rats indicated that hypoxic-ischemic damage in the brain was relieved following the intraventricular injection of BMSCs. These results suggested that apoptotic cells can be rescued during the pathological process of HIBD, providing a theoretical basis for the feasibility of effective BMSC administration.

The proliferation and differentiation potential of BMSCs may allow them to repair hypoxic-ischemic brain injury and provide a new therapeutic treatment method for neurological diseases. Magnetically targeted drug delivery represents a new model of drug delivery with potential clinical applications in the future. In this study, we found that the new magnet-targeted guidance method for SPIO-PLL-labeled BMSCs was effective for the treatment of HIBD in Sprague Dawley rats, and the therapeutic effects were better than those induced by the lateral ventricle or rat caudal vein injections of BMSCs. We also found that the IVIM MRI technique could be used to evaluate the efficacy of SPIO-PLL-labeled BMSCs for the treatment of HIBD *in vivo*. BMSCs have multipotent differentiation abilities, can be obtained from abundant sources, and feature low immunogenicity. In addition, BMSCs are associated with fewer ethical and operational difficulties in allotransplantation. The feasibility of BMSC transplantation for the treatment of hypoxic-ischemic brain injury provides a new potential method for exploring the treatment of neurological diseases. However, some problems remain. 1) The survival time and long-term safety of BMSCs after *in vivo* transplantation must be improved. 2) The best path and time window for migration remain to be determined. 3) The targeting and controllability of BMSCs therapy must be explored to determine the mechanisms for improving neurological function and neuronal signal transduction. 4) Specific cell surface markers that are capable of identifying BMSCs must be defined. The mechanisms through which BMSCs improve the functions of the host brain after transplantation following ischemic brain injury remain unclear. The exploration of these problems would promote revolutionary progress in the treatment of ischemic cerebrovascular disease.

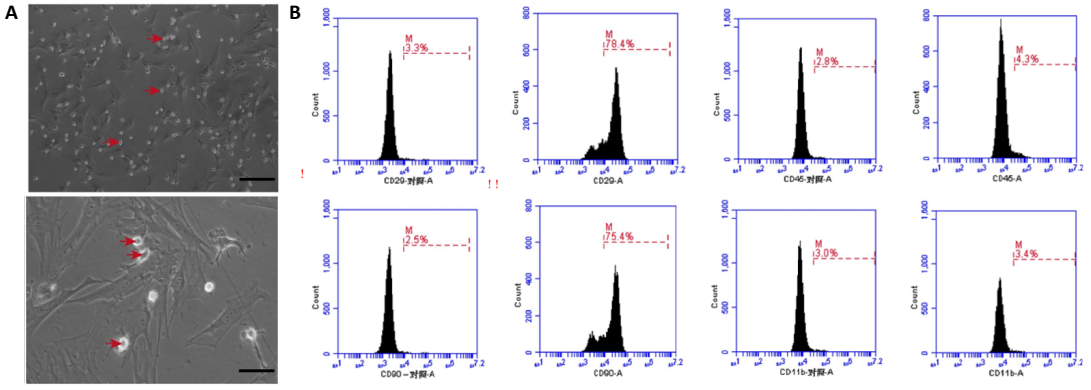

Figure 1 | Identification of bone marrow-derived mesenchymal stem cells.
(A) Morphology of bone marrow-derived mesenchymal stem cells (BMSCs, arrows) (magnification: upper 400×, lower 100×). Scale bars: 100 μm. (B) Identification of bone marrow-derived mesenchymal stem cells using flow cytometry. The BMSCs were CD29- and CD90-positive, and CD45- and CD11b-negative.

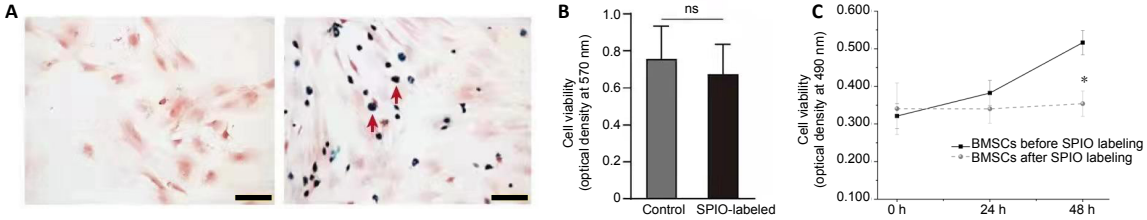

Figure 2 | Effects of SPIO-PLL labeling on the immediate survival and proliferation of BMSCs.
(A) Prussian blue staining of SPIO-PLL-unlabeled (left) and SPIO-PLL-labeled BMSCs (right, red arrows). Scale bars: 100 μm. (B) Cell proliferation examined by 3-(4,5-dimethylthiazol-2-yl)-2,5-diphenyltetrazolium bromide (MTT) after SPIO-PLL labeling. (C) Trypan blue staining of BMSCs before and after SPIO-PLL labeling. Data are expressed as the mean ± SD. The experiment was repeated three times. *P < 0.05 (Student's t-test). BMSCs: Bone marrow-derived mesenchymal stem cells; ns: not significant; PLL: poly-L-lysine; SPIO: superparamagnetic iron oxide nanoparticles.

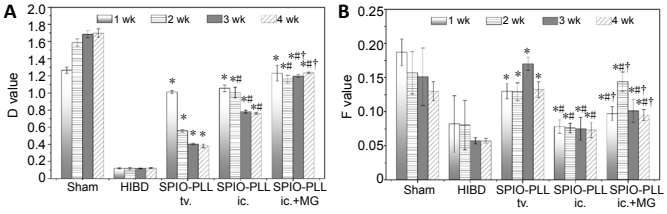

Figure 3 | The D (A) and F (B) values in the brains of HIBD rats treated with SPIO-PLL-labeled BMSCs at different time points after transplantation.
The D value represents the pure diffusion coefficient. The F value represents the perfusion fraction. Data are expressed as the mean ± SD (n = 16 per group). *P < 0.05, vs. HIBD group; #P < 0.05, vs. SPIO-PLL tv. group; †P < 0.05, vs. SPIO-PLL ic. group (one-way analysis of variance followed by Dunnett's $post\ hoc$ test). BMSCs: Bone marrow-derived mesenchymal stem cells; HIBD: hypoxic-ischemic brain damage; ic.: intraventricular injection; MG: magnetic guidance; PLL: poly L-lysine; SPIO: superparamagnetic iron oxide nanoparticles; tv.: tail vein injection.

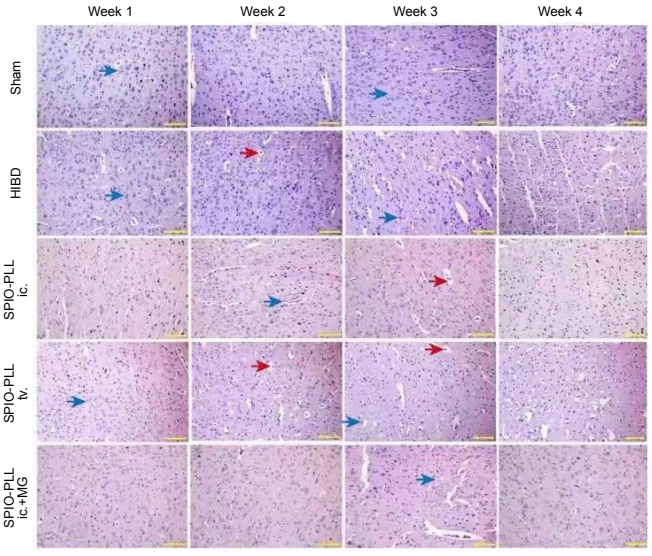

Figure 4 | Effects of SPIO-PLL-labeled BMSC transplantation on pathological damage in brain tissue of HIBD rats (hematoxylin/eosin staining).
Compared with the sham group, more extensive cerebral edema (red arrows) and inflammatory responses (blue arrows) were observed in the brains of HIBD rats from week 1 to week 4 after the operation. After SPIO-PLL-labeled BMSC injection, the degree of edema and cell death was reduced, and at week 4 after treatment, the degree of cerebral edema was significantly reduced, and cell apoptosis was barely observed. Moreover, the intraventricular injection of SPIO-PLL-labeled BMSCs showed better effects for the promotion of recovery from these pathological changes. Scale bars: 200 μm. BMSCs: Bone marrow-derived mesenchymal stem cells; HIBD: hypoxic-ischemic brain damage; ic.: intraventricular injection; MG: magnetic guidance; PLL: poly L-lysine; SPIO: superparamagnetic iron oxide nanoparticles; tv.: tail vein injection.

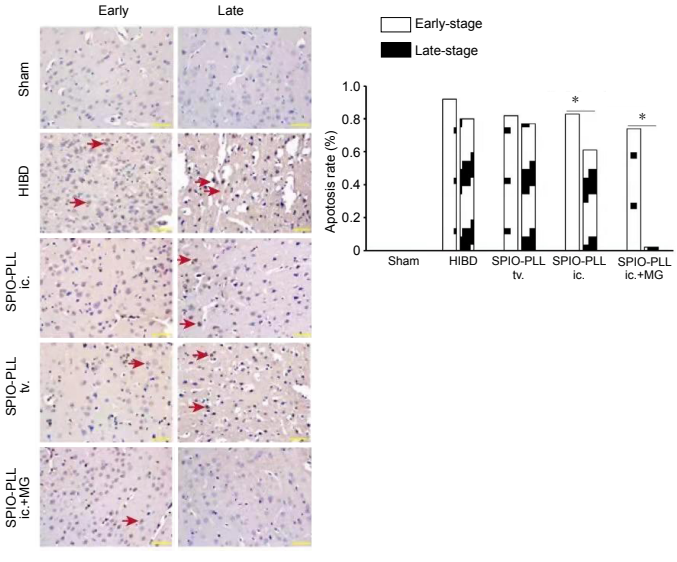

Figure 5 | Effect of SPIO-PLL-labeled BMSCs transplantation on apoptosis in brain tissue of HIBD rats (terminal deoxynucleotidyl transferase dUTP nick-end labeling staining).
In the HIBD group, a larger amount of cell death (red arrows) was observed compared with the sham group. Following the injection of SPIO-PLL-labeled BMSCs, the rates of cell apoptosis significantly decreased, and the SPIO-PLL ic. + MG group showed more therapeutic efficiency for decreasing cell death during the late stage. Early-stage: 1 and 2 weeks after injection; late-stage: 3 and 4 weeks after injection. Scale bars: 200 μm. Data are expressed as the mean (n = 16 per group) and were analyzed by one-way analysis of variance followed by Dunnett's $post\ hoc$ test. *P < 0.05. BMSCs: Bone marrow-derived mesenchymal stem cells; HIBD: hypoxic-ischemic brain damage; ic.: intraventricular injection; MG: magnetic guidance; PLL: poly-L-lysine; SPIO: superparamagnetic iron oxide nanoparticles; tv.: tail vein injection.

Author contributions: *Study conception and design: CS, JB, ZJL; intellectual content definition: CS, JB; experiment implementation: ADZ, HHC; data acquisition and analysis, statistical analysis, and manuscript preparation: ADZ; manuscript editing and review: CS, ADZ, JB. All authors contributed to this study and approved the final manuscript.*
Conflicts of interest: *The authors declare no conflict of interest.*
Financial support: *None.*
Institutional review board statement: *The study was approved by the Institutional Animal Care and Use Committee of The Second Hospital of Dalian Medical University, China (No. 2016-060) on March 2, 2016.*
Copyright license agreement: *The Copyright License Agreement has been signed by all authors before publication.*
Data sharing statement: *Datasets analyzed during the current study are available from the corresponding author on reasonable request.*
Plagiarism check: *Checked twice by iThenticate.*
Peer review: *Externally peer reviewed.*
Open access statement: *This is an open access journal, and articles are distributed under the terms of the Creative Commons Attribution-NonCommercial-ShareAlike 4.0 License, which allows others to remix, tweak, and build upon the work non-commercially, as long as appropriate credit is given and the new creations are licensed under the identical terms.*

References

Diamond MS, Springer TA (1993) A subpopulation of Mac-1 (CD11b/CD18) molecules mediates neutrophil adhesion to ICAM-1 and fibrinogen. J Cell Biol 120:545-556.

Evangelou N, Konz D, Esiri MM, Smith S, Palace J, Matthews PM (2000) Regional axonal loss in the corpus callosum correlates with cerebral white matter lesion volume and distribution in multiple sclerosis. Brain 123:1845-1849.

Federau C, Sumer S, Becce F, Maeder P, O'Brien K, Meuli R, Wintermark M (2014) Intravoxel incoherent motion perfusion imaging in acute stroke: initial clinical experience. Neuroradiology 56:629-635.

Fung SH, Roccatagliata L, Gonzalez RG, Schaefer PW (2011) MR diffusion imaging in ischemic stroke. Neuroimaging Clin N Am 21:345-377, xi.

Giannarini G, Petralia G, Thoeny HC (2012) Potential and limitations of diffusion-weighted magnetic resonance imaging in kidney, prostate, and bladder cancer including pelvic lymph node staging: a critical analysis of the literature. Eur Urol 61:326-340.

Hendrickx A, Bossuyt X (2001) Quantification of the leukocyte common antigen (CD45) in mature B-cell malignancies. Cytometry 46:336-339.

Jiang LJ, Xu ZX, Wu MF, Dong GQ, Zhang LL, Gao JY, Feng CX, Feng X (2020) Resatorvid protects against hypoxic-ischemic brain damage in neonatal rats. Neural Regen Res 15:1316-1325.

Krampera M, Cosmi L, Angeli R, Pasini A, Liotta F, Andreini A, Santarlasci V, Mazzinghi B, Pizzolo G, Vinante F, Romagnani P, Maggi E, Romagnani S, Annunziato F (2006) Role for interferon-gamma in the immunomodulatory activity of human bone marrow mesenchymal stem cells. Stem Cells 24:386-398.

Le Bihan D, Breton E, Lallemand D, Aubin ML, Vignaud J, Laval-Jeantet M (1988) Separation of diffusion and perfusion in intravoxel incoherent motion MR imaging. Radiology 168:497-505.

Lee J, Wecker A, Losordo DW, Yoon YS (2006) Derivation and characterization of bone marrow-derived multipotent stem cells. Exp Hematol 34:1602-1603.

Leyton L, Díaz J, Martínez S, Palacios E, Pérez LA, Pérez RD (2019) Thy-1/CD90 a bidirectional and lateral signaling scaffold. Front Cell Dev Biol 7:132.

Lidsky ME, Spritzer CE, Shortell CK (2012) The role of dynamic contrast-enhanced magnetic resonance imaging in the diagnosis and management of patients with vascular malformations. J Vasc Surg 56:757-764.e1.

Lin CQ, Chen LK (2020) Cerebral dopamine neurotrophic factor promotes the proliferation and differentiation of neural stem cells in hypoxic environments. Neural Regen Res 15:2057-2062.

Liu L, Oza S, Hogan D, Chu Y, Perin J, Zhu J, Lawn JE, Cousens S, Mathers C, Black RE (2016) Global, regional, and national causes of under-5 mortality in 2000-15: an updated systematic analysis with implications for the Sustainable Development Goals. Lancet 388:3027-3035.

Luciani A, Vignaud A, Cavet M, Nhieu JT, Mallat A, Ruel L, Laurent A, Deux JF, Brugieres P, Rahmouni A (2008) Liver cirrhosis: intravoxel incoherent motion MR imaging--pilot study. Radiology 249:891-899.

Miao Z, Jin J, Chen L, Zhu J, Huang W, Zhao J, Qian H, Zhang X (2006) Isolation of mesenchymal stem cells from human placenta: comparison with human bone marrow mesenchymal stem cells. Cell Biol Int 30:681-687.

Murnane JP, Sabatier L, Marder BA, Morgan WF (1994) Telomere dynamics in an immortal human cell line. EMBO J 13:4953-4962.

Pang Y, Turkbey B, Bernardo M, Kruecker J, Kadoury S, Merino MJ, Wood BJ, Pinto PA, Choyke PL (2013) Intravoxel incoherent motion MR imaging for prostate cancer: an evaluation of perfusion fraction and diffusion coefficient derived from different b-value combinations. Magn Reson Med 69:553-562.

Phillips AW, Johnston MV, Fatemi A (2013) The potential for cell-based therapy in perinatal brain injuries. Transl Stroke Res 4:137-148.

Sala E, Rockall A, Rangarajan D, Kubik-Huch RA (2010) The role of dynamic contrast-enhanced and diffusion weighted magnetic resonance imaging in the female pelvis. Eur J Radiol 76:367-385.

Shen CX, Stewart S, Wayner E, Carter W, Wilkins J (1991) Antibodies to different members of the beta 1 (CD29) integrins induce homotypic and heterotypic cellular aggregation. Cell Immunol 138:216-228.

Shinmoto H, Tamura C, Soga S, Shiomi E, Yoshihara N, Kaji T, Mulkern RV (2012) An intravoxel incoherent motion diffusion-weighted imaging study of prostate cancer. AJR Am J Roentgenol 199:W496-500.

Sun PZ, Wang Y, Mandeville E, Chan ST, Lo EH, Ji X (2014) Validation of fast diffusion kurtosis MRI for imaging acute ischemia in a rodent model of stroke. NMR Biomed 27:1413-1418.

van Velthoven CT, Kavelaars A, van Bel F, Heijnen CJ (2010) Mesenchymal stem cell treatment after neonatal hypoxic-ischemic brain injury improves behavioral outcome and induces neuronal and oligodendrocyte regeneration. Brain Behav Immun 24:387-393.

van Velthoven CT, Sheldon RA, Kavelaars A, Derugin N, Vexler ZS, Willemen HL, Maas M, Heijnen CJ, Ferriero DM (2013) Mesenchymal stem cell transplantation attenuates brain injury after neonatal stroke. Stroke 44:1426-1432.

Walton M, Connor B, Lawlor P, Young D, Sirimanne E, Gluckman P, Cole G, Dragunow M (1999) Neuronal death and survival in two models of hypoxic-ischemic brain damage. Brain Res Brain Res Rev 29:137-168.

Wang Y, Xu F, Zhang C, Lei D, Tang Y, Xu H, Zhang Z, Lu H, Du X, Yang GY (2011) High MR sensitive fluorescent magnetite nanocluster for stem cell tracking in ischemic mouse brain. Nanomedicine 7:1009-1019.

Westerweel PE, Verhaar MC (2008) Directing myogenic mesenchymal stem cell differentiation. Circ Res 103:560-561.

Xue LL, Wang F, Niu RZ, Tan YX, Liu J, Jin Y, Ma Z, Zhang ZB, Jiang Y, Chen L, Xia QJ, Chen JJ, Wang TH, Xiong LL (2020) Offspring of rats with cerebral hypoxia-ischemia manifest cognitive dysfunction in learning and memory abilities. Neural Regen Res 15:1662-1670.

Yager JY (2004) Animal models of hypoxic-ischemic brain damage in the newborn. Semin Pediatr Neurol 11:31-46.

Yıldız EP, Ekici B, Tatlı B (2017) Neonatal hypoxic ischemic encephalopathy: an update on disease pathogenesis and treatment. Expert Rev Neurother 17:449-459.

Zuo L, Feng Q, Han Y, Chen M, Guo M, Liu Z, Cheng Y, Li G (2019) Therapeutic effect on experimental acute cerebral infarction is enhanced after nanoceria labeling of human umbilical cord mesenchymal stem cells. Ther Adv Neurol Disord 12:1756286419859725.

C-Editor: Zhao M; S-Editors: Yu J, Li CH; L-Editors: Giles L, Yu J, Song LP; T-Editor: Jia Y